Taylor & Francis
Taylor & Francis Group

Inland Waters

ISSN: 2044-2041 (Print) 2044-205X (Online) Journal homepage: http://www.tandfonline.com/loi/tinw20

Effect of southern climate modes and variations in river discharge on lake surface area in Patagonia

Facundo Scordo, Gerardo M. E. Perillo & M. Cintia Piccolo

INLAND WATERS
https://doi.org/10.1080/20442041.2018.1487118

Effect of southern climate modes and variations in river discharge on lake surface area in Patagonia

Facundo Scordo,[a,b] Gerardo M. E. Perillo,[a,c] and M. Cintia Piccolo[a,b]

[a]CONICET - Instituto Argentino de Oceanografía, Bahía Blanca, Buenos Aires, Argentina; [b]Departamento de Geografía y Turismo, Universidad Nacional del Sur, Bahía Blanca, Buenos Aires, Argentina; [c]Departamento de Geología, Universidad Nacional del Sur, Bahía Blanca, Buenos Aires, Argentina

ABSTRACT
Multiple regressions, wavelet spectra, and Fourier spectra were employed to analyze fluctuations in the surface areas of 2 Patagonian lakes during 1998–2015 and relate these to fluctuations in precipitation, evaporation, river discharge, and 2 southern climate modes, the Antarctic Oscillation (AAO) and El Niño Southern Oscillation, expressed in terms of the Southern Oscillation Index (SOI). Multiple regression analysis suggested that discharge was the primary driver of interannual lake area variations. Cross-spectrum analysis demonstrated a maximum significant correlation between river discharge and both AAO and SOI indices at annual and interannual timescales (2–3 yr). During 1998–2015, the annual discharge signal was related to both the AAO annual and every 2 year signals. When a strong La Niña (positive SOI) event occurred, however, river discharge was significantly reduced, resulting in a decrease in lake surface area.

ARTICLE HISTORY
Received 9 January 2017
Accepted 1 April 2018

KEYWORDS
AAO; lake surface area; Patagonian plains region; river discharge; SOI

Introduction

Climatic variability affects temperature, precipitation, wind, and hydrological processes, resulting in variable runoff patterns (Milly et al. 2005, Park et al. 2010, Beniston and Stoffel 2014). The response of hydrological systems can change significantly, generating a threat to arid and semiarid regions (Williamson et al. 2009), as in the case of Argentine Patagonia.

Lakes and reservoirs are highly sensitive to climate variability and change (Williamson et al. 2008, 2009, Park et al. 2010, Shimoda et al. 2011), but their responses can vary depending on the physical characteristics of the lakes. Shallow lakes are especially sensitive to climate-related effects such as variations in temperature, wind intensity, precipitation, and flow regimes (George et al. 2007, Whitehead et al. 2009, Williamson et al. 2009, Woolway et al. 2017).

Numerous studies have demonstrated how lake size influences other lake characteristics. For example, lake size affects the relative contributions of wind and convective mixing to the gas transfer coefficient (Read et al. 2012). Small lakes are often well sheltered from the wind and consequently experience lower wind speeds than larger lakes with a greater fetch (Hondzo and Stefan 1993), and thus the amount of mixing in a lake varies with surface area changes. Lake size can also influence the magnitude of diurnal heating and cooling in lakes (Woolway et al. 2016), which in turn influences the gas transfer coefficient (Holgerson et al. 2017). Moreover, the surface water temperature of the smaller lakes in the northeastern United States has been increasing more rapidly than that of larger lakes in recent decades (Torbick et al. 2016). A comprehensive review of the influence of lake size on lake ecology has been provided by Downing (2010). Understanding why lake surface area varies is crucial, especially in an era of climate change. A strong relationship exists between lake surface area variations and climatic and hydrological variables such as temperature, precipitation, and evaporation (Ye et al. 2008, Yan and Zheng 2015). Thus, changes in lake surface area can be viewed as indicators of climate variability (Shi and Ren 1990, Ye et al. 2008, Yan and Zheng 2015).

The Argentine Patagonia region (located in the southern part of South America) is a semiarid zone of considerable interest because of its high sensitivity to climate variability. Patagonian lakes are the largest and deepest waterbodies in South America (Quirós and Drago 1999), and water resources in this region are critically affected by climate variability (Dore 2005, Compagnucci and Araneo 2007, Araneo and Compagnucci 2008). During the 20th century, the increase in temperature

CONTACT Facundo Scordo fscordo@criba.edu.ar

and decrease in snowfall have resulted in glacier recession and regional hydrological changes (Masiokas et al. 2008, Pasquini et al. 2008). These changes illustrate how climate variability has become a significant threat to both the quantity and quality of freshwater resources in the region.

Studies on the influence of climatic factors and regional climatic modes, such as El Niño Southern Oscillation (ENSO) and the Antarctic Oscillation (AAO), on the hydrology of Argentine Patagonian rivers and lakes between 45°S and 50°S have yielded contradictory results. For example, Pasquini and Depetris (2007) demonstrated that the discharge of Patagonian rivers between 45°S and 50°S fluctuates at a frequency similar to that of El Niño (2–7 yr), and river discharge in this area maintains a simultaneous relationship with sea surface temperature in the El Niño 3 + 4 area (Compagnucci and Araneo 2007). Moreover, during strong El Niño events, the mean zonal wind speed over the Pacific Ocean from 50°S to 55°S decreases, reducing precipitation on the west coast of Chile between 45°S and 55°S by 10–20% (Schneider and Gies 2004). From other studies, river discharge fluctuations in this area are related to the Southern Annular Mode, with little influence of ENSO events (Lara et al. 2015), whereas lakes in this area are probably more dependent on local forcing factors (Pasquini et al. 2008). Thus the Argentine Patagonia region, located on the eastern side of the Andes between 45°S and 50°S, seems to be a transitional zone where both ENSO, expressed in terms of the Southern Oscillation Index (SOI), and AAO likely play a major role in lake and river hydrology.

Musters Lake (45°26′S, 69°11′W) and Colhué Huapí Lake (45°32′S, 68°45′W) form the terminal stage of the Senguer River basin in Argentine Patagonia. Despite being separated by <15 km, the physical characteristics of the 2 lakes vary broadly. Musters is a relatively deep lake, whereas Colhué Huapí is shallow (Quirós et al. 1983). In 1998–2002, marked fluctuations were observed in the size of Colhué Huapí Lake, which reached its smallest area (105 km^2) in 2001. Some studies projected that the lake could disappear, mostly because water used for crop irrigation has intensified during drought seasons (Coronato 2003, Tejedo 2003).

The most productive austral valley of the world (Sarmiento Valley) is located south of Musters and Colhué Huapí lakes, occupying 20% of the area surrounding the lakes. Crops (primarily lucerne), fruits, and vegetables are grown there. Oil drilling facilities and cherry orchards located near the lakes use large quantities of water. These 2 lakes, particularly Musters Lake, are strategically important as a water source for the local and regional communities. An aqueduct from Musters Lake supplies 150 000 m^3/d of water to 350 000 inhabitants (Valladares 2004).

We investigated the interannual fluctuations in the surface areas of Musters and Colhué Huapí lakes as related to precipitation, evaporation, river discharge, and southern climate modes (AAO and SOI) during 1998–2015. The lack of detailed physical monitoring of these lakes did not allow variations in lake volume to be analyzed, but changes in lake surface area could be studied with satellite imagery. We hypothesized that these lakes are subject to natural interannual fluctuations in their surface area resulting from variations in river discharge and climate, which in turn are related to both ENSO and AAO climate modes.

Study site

Musters Lake and Colhué Huapí Lake (Fig. 1), the largest natural extra-Andean waterbodies in Chubut province (González Díaz and Di Tomasso 2014), are situated to the east of the Andes in the Patagonian plains, separated by a north–south ridge that reaches an elevation of 600 m a.s.l. Musters is a narrow (width 12 km, length 40 km), deep (maximum depth 38.5 m) lake with a north–south orientation (Quirós et al. 1983). It is of tectonic origin and is surrounded by land of high elevation (1200 m a.s.l.) on its western, northern, and central-eastern coasts. The southern shore is part of a former delta of the Senguer River. Colhué Huapí is a large (width 23 km, length 50 km) shallow (maximum depth 5.5 m) lake (Quirós 1988) that, although also created by tectonic processes, was reshaped by eolian and fluvial activity (González Díaz and Di Tomasso 2014). Except for the northern coast (500 m), most of the lake has flat shores, and its western and southern coasts also form part of the Senguer River delta. The physical differences between the 2 lakes are important during periods of water shortage because the shallower lake is more affected by the wind and increased evaporation (Tejedo 2003).

The Senguer River originates in the Andes, with most of its tributaries at its headwaters. The river flows 350 km before finally discharging into Musters and Colhué Huapí lakes on the Patagonian plains (Fig. 1). The Senguer River has a maximum flow rate in October and November from snowmelt in its upper basin (Bruniard 1992).

The Senguer River basin is endorheic and flows into Musters Lake on its southern coast. Part of the river diverges to the east 50 m toward the Falso Senguer River before reaching Musters Lake. The Falso Senguer River discharges into Colhué Huapí Lake on its west coast (Fig. 1). Currently, Musters and Coluhé Huapí

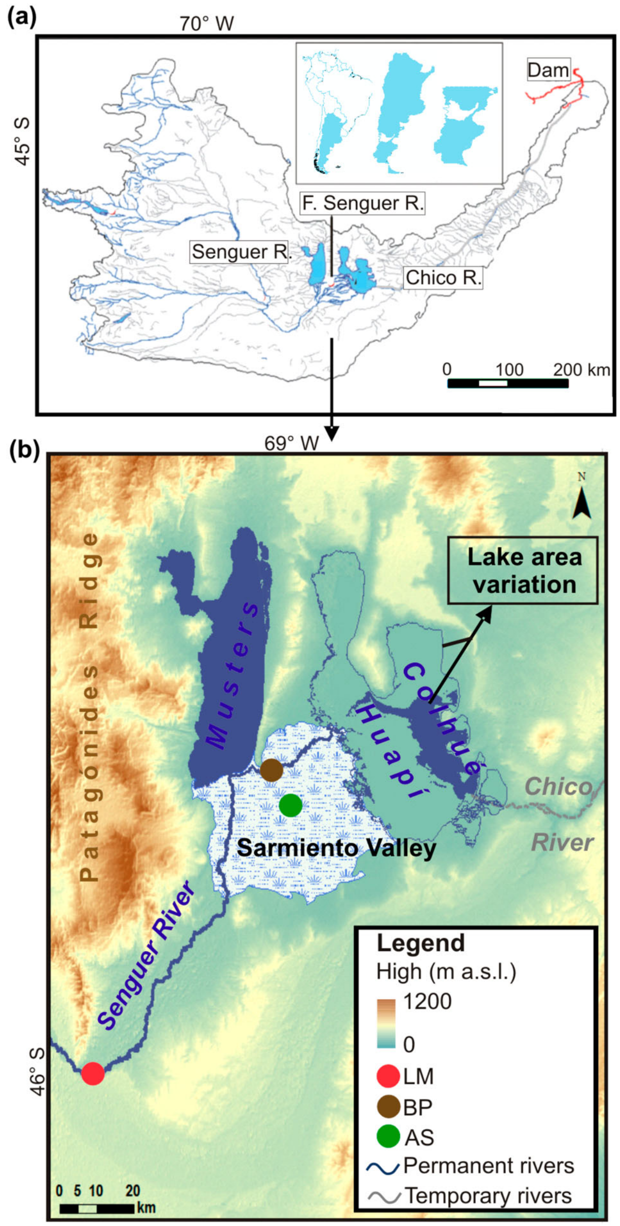

Figure 1. General description of the study site. (a) Senguer River basin; (b) Musters Lake, Colhué Huapí Lake, and the hydrological (LM, BP) and meteorological (AS) monitoring stations within the Senguer River basin. The terrain on the western, northern, and east-central coasts of Musters Lake is elevated (up to 1200 m a.s.l.) but low and smooth around the shores of Colhué Huapí Lake.

lakes have no natural outflow and lose water only through evaporation. Colhué Huapí Lake used to have a natural outflow on its east coast, the Chico River, once a tributary of the Chubut River, which ends in the Atlantic Ocean. Changes in climatic conditions have modified the geomorphology around Colhué Huapí Lake, however, and since the 1950s the Chico River has been a dry channel only partly fed by local rainfall (Tejedo 2003, Valladares 2004, Scordo et al. 2017).

A strong precipitation gradient exists across the basin, from the Andes in the west (nearly 1200 mm/yr) to the lakes in the east (100–200 mm/yr). Precipitation has 2 effects on the lake water inflows. In the upper basin, rainfall is the source of the Senguer River discharge, while precipitation over the lakes is a direct inflow at the lower basin. The low (local) rainfall in the lower basin does not influence the Senguer River discharge because the surrounding lake area is dry and the precipitation quickly infiltrates. Mean annual temperature is 8 °C with large thermal amplitudes. The wind is a significant meteorological factor because of its intensity and persistence. The prevailing wind direction is from the west and southwest, with high speeds (30 km/h) and gusts of 100 km/h (Valladares 2004). Evaporation in this region is high (1800 mm/yr).

Although some regional studies have analyzed the effect of southern climate modes on Patagonian rivers, the joint effect of SOI and AAO in the region where Musters and Colhué Huapí lakes are located has not yet been well studied. According to recent studies (Aravena and Luckman 2009), south of 40°S the rainfall and snow deposition in the Andes region is affected mostly by AAO variations, whereas the SOI is highly correlated with the rainfall in the Patagonian plains region, with 3- to 7-year oscillation modes (Aceituno 1988, Aravena and Luckman 2009). Fluctuations in the Senguer River discharge have been associated with variations in the ENSO cycle (Compagnucci and Araneo 2007).

Methods

Lake surface area delineation

Landsat (5 TM, 7 ETM+, and 8 OLI) images were used to analyze interannual fluctuations in lake surface area but could not be used to study intraannual fluctuations. Although the Landsat images have a temporal resolution of 16 d, not all the available images were useful because of a high percentage of cloud cover and the Scan Line Error of Landsat 7 images (since 2003). These images are freely available, however, and have a reasonably high spatial resolution (30 × 30 m), a critical consideration for this study because high spatial resolution is needed to analyze the low areal variation common in deep lakes.

One satellite image per year was processed to analyze the interannual lake area fluctuations. We analyzed 18 Landsat images for 1998–2015, using mostly summer images from December and January. The highest river discharge occurred during spring (Oct and Nov), and its effects on lake area extension can be best observed during summer. Additionally, summer images contained less cloud cover and were the only ones available for each year analyzed in this study. The images corresponded to Landsat Higher Level products (Path 229 and Row 92), downloaded from US Geological Survey (http://earthexplorer.usgs.gov). Each image included surface reflectance data. Specific details about how the Landsat Level 1 products are corrected and converted into surface reflectance data can be found at https://landsat.usgs.gov/landsat-surface-reflectance-high-level-data-products.

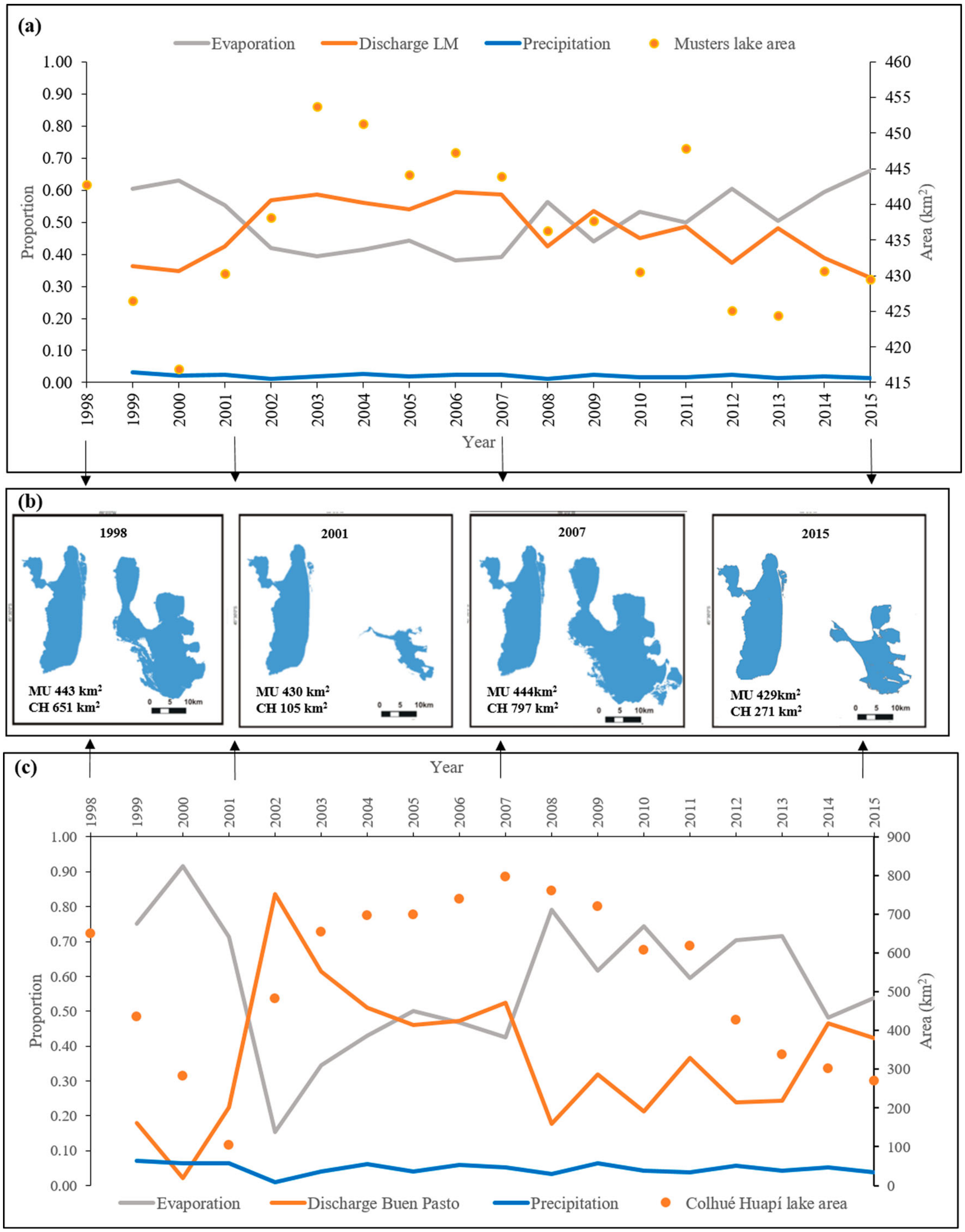

Figure 2. Time series of the surface areas of Musters (MU) and Colhué Huapí (CH) lakes (1998–2015), along with the discharge, precipitation, and evaporation as proportions of the total water flow for (a) Musters and (b) Colhué Huapí lakes. Three different periods of lake area changes can be defined for Colhué Huapí Lake. From 1998 to 2001 the lake area decreased from 651 to 105 km^2, from 2001 to 2007 it increased to 797 km^2, and from 2007 to 2015 it decreased again to 271 km^2 (b). Precipitation = annual precipitation multiplied by lake area. Evaporation = annual evaporation multiplied by lake area.

To differentiate water from other types of land cover, a red-green-blue (RGB) band combination (near infrared, short wave infrared, red) was applied to the Landsat images (Landsat 5 and 7: bands 4-5-3; Landsat 8: bands 5-6-4), a band combination that has accurately distinguished water from other types of land cover (NASA 1999, Horning 2004, Chuvieco 2010). Lake areas were obtained by a supervised classification (maximum likelihood), based on a defined region of interest (ROI), and vectorization made with ENVI 4.7 software (ENVI 2010). A raster calculator tool from ArcGIS 10.0 (ArcGIS 2010) was employed to calculate lake surface area (Fig. 2). A comparison of the summer images showed the degree of lake surface change over time.

Annual time series of hydrological and meteorological variables

Time series of mean monthly data (averages of daily data) were provided by Subsecretaría de Recursos Hídricos de la Nación (SSRH 2016; http://www.hidricosargentina.gov.ar/acceso_bd.php) from Los Molinos (LM; 45°59′24″S, 69°30′0″W) and Puente Camino Buen Pasto (BP; 45°33′36″S, 69°3′36″W) discharge stations and from Aeroclub Sarmiento (AS; 45°34′12″S, 69°4′48.9″W) meteorological station (Fig. 1). The data from the LM discharge station, located before the Senguer River reaches Musters Lake, were employed in the Musters area analysis. The BP station is located in the Falso Senguer River before Colhué Huapí Lake; the data from this station were used in the Colhué Huapí area analysis. The data from meteorological station AS, situated between the 2 lakes, were employed in the study of both lakes (Fig. 1).

Total annual discharge (m^3/yr), total annual evaporation (mm/yr), and total annual precipitation (mm/yr) were calculated. The descriptive statistics of each time series of discharge, precipitation, and evaporation were calculated and briefly described to better understand the natural conditions of the area.

Multiple linear regression between lake surface area and discharge, precipitation and evaporation

Total annual lake water inflows and outflows were calculated for Musters and Colhué Huapí lakes. Inflows are the annual river discharge (m^3/yr) into each lake and annual (local) precipitation (m^3/yr) over each lake (annual precipitation multiplied by lake area). Local precipitation does not influence the discharge because the surrounding area is dry and the precipitation is low; thus, it quickly infiltrates, and the volume reaching the lakes is negligible. The only outflow from both lakes is the annual evaporation (m^3/yr) from the lake surfaces (annual evaporation multiplied by lake surface area). The proportion of these flows (discharge, local precipitation over the lake and lake evaporation) was calculated with respect to total flow to understand their relative importance (Fig. 2). Musters Lake also has an artificial outflow from an aqueduct active since 1965. Although no official data are available, the estimated outflow from the aqueduct is 1.7 m^3/s, equivalent to 47.3×10^6 m^3/yr.

The annual series for each variable was used to calculate a multiple regression between lake surface area and discharge, precipitation, and evaporation. Each variable has a seasonal component that was not analyzed in this study because it is only relevant to intraannual fluctuations; analysis of intraannual fluctuations was not possible because Landsat satellite images were unavailable.

To study the complexity of the interannual lake area fluctuations, standard multiple regressions were calculated between the annual series of lake area (A_{t0}) in a given year as the dependent variable, and the series of total annual discharge (Q_{t-1}), annual precipitation (Ppt_{t-1}) over the lake, and annual lake evaporation (ET_{t-1}) in the year immediately previous to that year as independent variables (Table 1). The outflow from Musters Lake through the aqueduct was not included because it was assumed to be constant over the study period and thus yields no information relevant to variations in lake surface area.

Each independent variable in the multiple regressions has an associated beta coefficient (β) indicating how much the standard deviation of the dependent variable increases when the independent variable is increased by 1 standard deviation (SD), assuming other variables in the model are unchanged. The net values of β are a measure of the total effect of the independent variables, so the independent variable with the highest net value

Table 1. Description of the variables used in the multiple regressions calculated between annual series of lake area (A_{t0}) as dependent variable, and series of total annual discharge (Q_{t-1}), annual precipitation (Ppt_{t-1}) over the lake, and annual lake evaporation (ET_{t-1}) from the year immediately preceding the current lake area, as independent variables.

Variables	Units	Description
A_{t0}	km^2	Lake area at time t = 0
Q_{t-1}	m^3/s	Total annual discharge in the year immediately preceding A_{t0}
Ppt_{t-1}	m^3/s	Total annual precipitation (m) in the year immediately preceding A_{t0} multiplied by the lake area (m^2) in the year immediately preceding A_{t0}
ET_{t-1}	m^3/s	Total annual evaporation (m) in the year immediately preceding A_{t0} multiplied by the lake area (m^2) in the year immediately preceding A_{t0}

of β is the one with the greatest total effect over the dependent variable. Thus, in this study, the analysis of net values of β showed the relative importance of discharge, precipitation, and evaporation for the variability of lake surface area.

Standard multiple regressions were calculated using 10-year data from 1999 to 2008.

The model fit for the lake surface area was evaluated using the Nash-Sutcliffe model efficiency index (NSE; Nash and Sutcliffe 1970), calculated by comparing the observed lake surface area data from satellite images between 2009 and 2015 against the model predictions for the same years. The modeled surface area was calculated using the coefficients of the multiple regression analysis for 1999–2008 for each variable (discharge, evaporation, and precipitation). All the statistical analyses were performed with a confidence level of 95%.

Spectral procedures

Spectral procedures were applied to study the effect of the AAO and SOI on river discharge and lake surface area. Monthly data of AAO and SOI anomalies were downloaded from the National Oceanic and Atmospheric Administration (http://www.cpc.ncep.noaa.gov/data/indices). We focused on the correlation between the discharge at station BP and the AAO, and the discharge at station BP and the SOI. River discharge and the AAO and SOI periodicities were analyzed by applying 2 spectral procedures to the mean monthly data series: wavelet analysis (Morlet wavelet method) and the fast Fourier transform (FFT; Welch method with a Hamming window). Although analyzing the individual spectrum of each variable was useful, we were also interested in the relationship between river discharge and the 2 climate modes. Thus, the cross-spectra of the time series were calculated with both spectral procedures. Deseasonalized monthly mean series were used, obtained by subtracting the overall monthly historical means from the individual monthly means.

Wavelet analysis (employing the Wavelet Toolbox in the MATLAB 9.0 environment; MATLAB 2016) was applied to the time series (Torrence and Compo 1998, Grinsted et al. 2004) The time series used were 228 months long, from 1996 to 2014, allowing us to identify the most important periodicities of the spectrum and when they occurred. We also calculated cross-wavelet transforms, which allowed identification of regions in time-frequency space where the time series show high common power.

Wavelet analysis offers several advantages over traditional Fourier analysis (Lau and Weng 1995, Pasquini and Depetris 2007, Bhon et al. 2016). It allows the use of long time intervals, where precise low-frequency information is required, and shorter regions where high-frequency information is required, making it suitable for signals with both low-frequency/long-duration components and high-frequency/short-duration components, as found in some environmental time series. Another important distinction between wavelet analysis and traditional spectral analysis is that wavelet analysis is not limited to using sinusoidal analyzing functions. Rather, a large selection of localized waveforms, known as wavelet functions, can be used. For that reason, among others, wavelet analysis has become increasingly popular in a range of scientific disciplines, particularly in atmospheric and oceanic sciences, and more recently in limnology (Woolway et al. 2014, Bruesewitz et al. 2015, Carey et al. 2016). Because our interest was in capturing the oscillatory behavior of a time series consisting of unknown frequencies, and because we expected the wavelet spectra at adjacent times to be highly correlated, a Morlet wavelet was employed, which yields more robust results compared to other mother wavelets (Chopra and Marfurt 2015).

We were also particularly interested in analyzing the phase shift (time lag) between discharge and both southern climate modes (AAO and SOI). Thus, despite the advantages of wavelet analysis, the FFT cross-spectra were also analyzed. The FFT cross-spectra allowed the phase shift between time series to be calculated for periodicities with high cross-coherence. Phase shifts between discharge and both southern climate modes were analyzed for periodicities at which the squared coherency of the time series exceeded 0.75. Data for 204 months were available between 1998 and 2015. To increase confidence levels for the FFT analysis, the monthly series used were therefore 1987–2014 (336 months). All FFT analyses were performed using the software Statistica 7 (Statistica 2002).

Results

Time series of annual values

Lake surface area

During the study period, the interannual fluctuation in lake surface area (summer values) was clear, and most evident for Colhué Huapí Lake because of its shallow depth. The mean surface area (mean [SD]) of Colhué Huapí Lake was 534 (207) km^2; its minimum was 105 km^2 (reached during 2001), and its maximum was 797 km^2 (reached during 2007). The mean surface area of Musters Lake was 437 (10) km^2; its minimum was 417 km^2 (reached during 2000), and its maximum was 454 km^2 (reached during 2003). For Colhué Huapí, 3

Table 2. Mean, standard deviation (SD), minimum and maximum of total annual precipitation, total annual evaporation, mean annual discharge at Los Molinos (LM) and Puente Camino Buen Pasto (BP) stations, and the surface areas of Colhué Huapí (CH) and Musters (MU) lakes.

	Precipitation mm/yr	Evaporation mm/yr	Discharge BP m^3/yr	Discharge LM m^3/yr	CH area (km^2)	MU area (km^2)
Mean	160	1756	22	51	534	437
SD	57	155	14	16	207	10
Min	71	1527	1	28	105	417
Max	315	2087	46	79	797	454

different periods of lake surface area change could be defined. From 1998 to 2001 the lake surface area decreased from 651 km^2 to its minimum (105 km^2); from 2001 to 2007 it increased to its maximum (797 km^2); and from 2007 to 2015 it decreased again to 271 km^2 (Fig. 2, Table 2). During the same period, the surface area of Musters fluctuated by <10% around its long-term mean (Fig. 2, Table 2).

Total annual evaporation

Total annual evaporation varied between a minimum of 1527 mm and a maximum of 2087 mm, with a mean value of 1756 (155) mm (Table 2). The highest evaporation occurred before or during a period of lake area decrease (1998 and 2009 [2087 and 1909 mm, respectively]) and the lowest before or during a period of lake area increase (2003 [1527 mm]).

Total annual precipitation

Total annual precipitation varied between a minimum of 71 mm and a maximum of 315 mm, with a mean value of 160 (57) mm (Table 2). The highest precipitation occurred before or during a period of lake area increase (1997 and 2005 [314 and 280 mm, respectively]) and the lowest before or during a period of lake area decrease (2007 and 2012 [71 and 103 mm, respectively]).

Mean annual discharge

Mean discharge values measured at the BP hydrological station were lower than those measured at the LM station because most of the Senguer River water that passes through the LM station flows into Musters Lake (or is used for agricultural activities), and only part of this discharge reaches the BP station via the Falso Senguer River (Fig. 1). Despite the difference in mean discharge (LM: 51 m^3/s; BP: 22 m^3/s), the discharge fluctuation patterns at both stations were similar. The lowest discharge values (LM: 28 m^3/s; BP: 1 m^3/s) occurred before or during a period of lake area decrease and the highest values (LM: 79 m^3/s; BP: 43 m^3/s) during a period of lake area increase (Table 2).

Components of net flow

Discharge, precipitation, and evaporation represented different contributions to the net water flow (discharge + precipitation - evaporation) for each lake. The annual precipitation over the lake (m^3/year; annual precipitation in m/yr multiplied by lake area) made the lowest contribution to the net flow for both lakes (<0.1%). For Colhué Huapí, the proportion of the net flow accounted for by precipitation reached higher values (0.07) than for Musters (0.03), and these higher values occurred during periods of increasing lake area.

The proportion of the net water flow accounted for by annual evaporation from the lake (annual evaporation in m/yr multiplied by lake area) was between 0.4 and 0.6 m^3/yr for Musters and between 0.15 and 0.9 m^3/yr for Colhué Huapí. The fluctuation was greater for Colhué Huapí. Evaporation from Colhué Huapí represented the highest proportion of the net flow during periods of decreasing lake surface area and the lowest proportion during periods of increasing lake surface area.

Annual discharge findings were opposite those for evaporation in both lakes, varying between 0.3 and 0.6 m^3/yr for Musters and between 0.18 and 0.84 m^3/yr for Colhué Huapí. The fluctuation was greater for Colhué Huapí. Annual discharge represented the highest proportion of the net flow during periods of lake area increase and the lowest proportion during periods of lake area decrease.

Summarizing, the annual discharge and annual precipitation (inflows) accounted for the highest proportion of the net flow during periods of lake area increase and the lowest proportion during periods of lake area decrease, whereas the opposite was true for the annual evaporation (outflow). The variability of these flows seems to correspond with the variability of lake surface area.

Multiple regression analysis for lake surface area

Standard multiple regressions of the annual time series of lake surface area (A_{t0}) as the dependent variable, and time-series of the total annual discharge (Q_{t-1}), annual precipitation (Ppt_{t-1}) over the lake, and annual lake evaporation (ET_{t-1}) measured 1 year previous to the lake

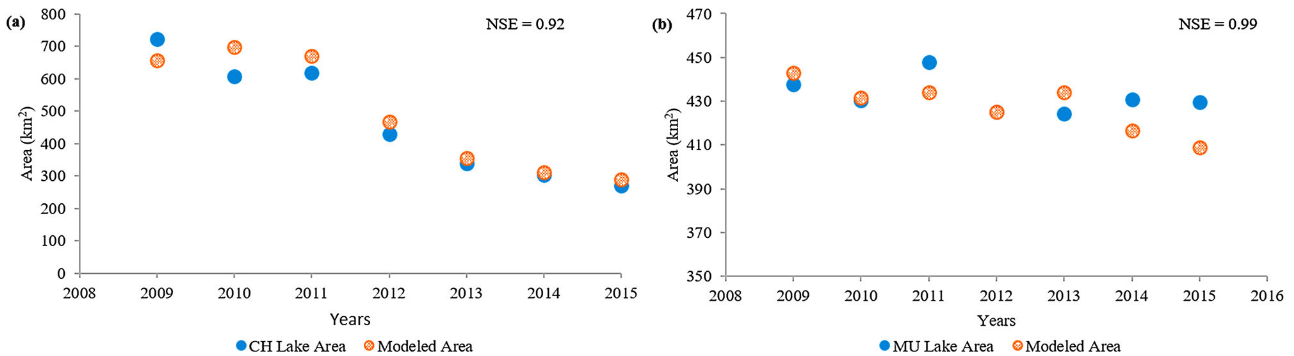

Figure 3. (a) Observed and modeled surface area of Colhué Huapí Lake (CH) for 2009–2015; (b) observed and modeled area of Musters Lake (MU) for the same period. The model fit for both lake areas was tested using the Nash-Sutcliffe model efficiency index (NSE). The modeled area was calculated from the coefficients of the multiple regression analysis for 1999–2008.

surface area as independent variables, were calculated based on 10 years of data from 1999 to 2008. For both lakes, a highly significant relationship was found. For Musters, the regression indicated that ~74% (adjusted $R^2 = 0.74$; $p < 0.001$) of the variance of the lake surface area could be accounted for by a linear combination of the independent variables. For Colhué Huapí, the equivalent figure was 86% (adjusted $R^2 = 0.86$; $p < 0.001$). The model fit for lake surface area was evaluated using the NSE by comparing observed lake surface area data from satellite images between 2009 and 2015 with model predictions for the same years. For both lakes, the coefficients of the multiple regression well-predicted their area: for Colhué Huapí the NSE was 0.92 and for Musters NSE was 0.99 (Fig. 3).

Net values of the beta coefficient (β) show the importance of the variables in a linear multiple regression. The variable that best described surface area fluctuations for both lakes was river discharge (β = 1.1 for Colhué Huapí and β = 0.80 for Musters). Evaporation and precipitation were also highly significant for Colhué Huapí ($\beta = 0.97$; $p < 0.001$; $\beta = 0.58$; $p < 0.05$) but not for Musters.

Although the model predicted the surface area variations of both lakes well, the correlation coefficient for Colhué Huapí was higher than the correlation coefficient for Musters. The lake surface area variation not explained by the multiple regression might be associated with the effect of groundwater and water reaching the lakes through other surface channels, which were not included in this regression due to lack of data. Also, the uncertainty associated with the pixel definition of the Landsat image (30 × 30 m) likely has a more significant effect in the case of Musters because of its geomorphology. Moreover, ~1.5 m^3/s of water from Musters is pumped into an aqueduct, an effect not included in the analysis based on the assumption that the outflow from the lake toward the aqueduct would be relatively constant and would therefore not affect the variability of the lake surface area.

Relationship of fluctuations in lake surface area to fluctuations in discharge and in the AAO and SOI indexes

For both lakes, changes in the surface area were mostly due to changes in discharge. Therefore, we hypothesized that regional or global events that affect the discharge would also affect lake surface area. We focused attention on Colhué Huapí Lake because its surface area underwent pronounced changes during the study period. Two spectral procedures (wavelet analysis and FFT) were applied to analyze the correlation between the discharge at the BP hydrological station and both the AAO and SOI.

Wavelet analysis

For the discharge series, wavelet analysis revealed a maximum energy in the annual periodicity, but this peak did not cover the entire study period; between 1998 and 2000 and between 2010 and 2013, the annual discharge signal disappeared. These periods (1998–2000 and 2010–2013) preceded 2001 and 2015, respectively, when the lake surface area reached its minimum sizes (Fig. 4a).

Cross-wavelets between the discharge at BP and the AAO series showed a significant correlation maximum at the annual periodicity. This signal was strong during most of the timeframe covered by this study. During 1999–2000 and 2006–2012, however, the correlation at the annual periodicity disappeared, and during 2006–2012 a significant correlation at a periodicity of about 2–3 yr appeared (Fig. 4b). Cross-wavelets between the discharge at BP and the SOI series presented a different behavior. Although the cross-wavelets also revealed a significant correlation maximum at the annual periodicity,

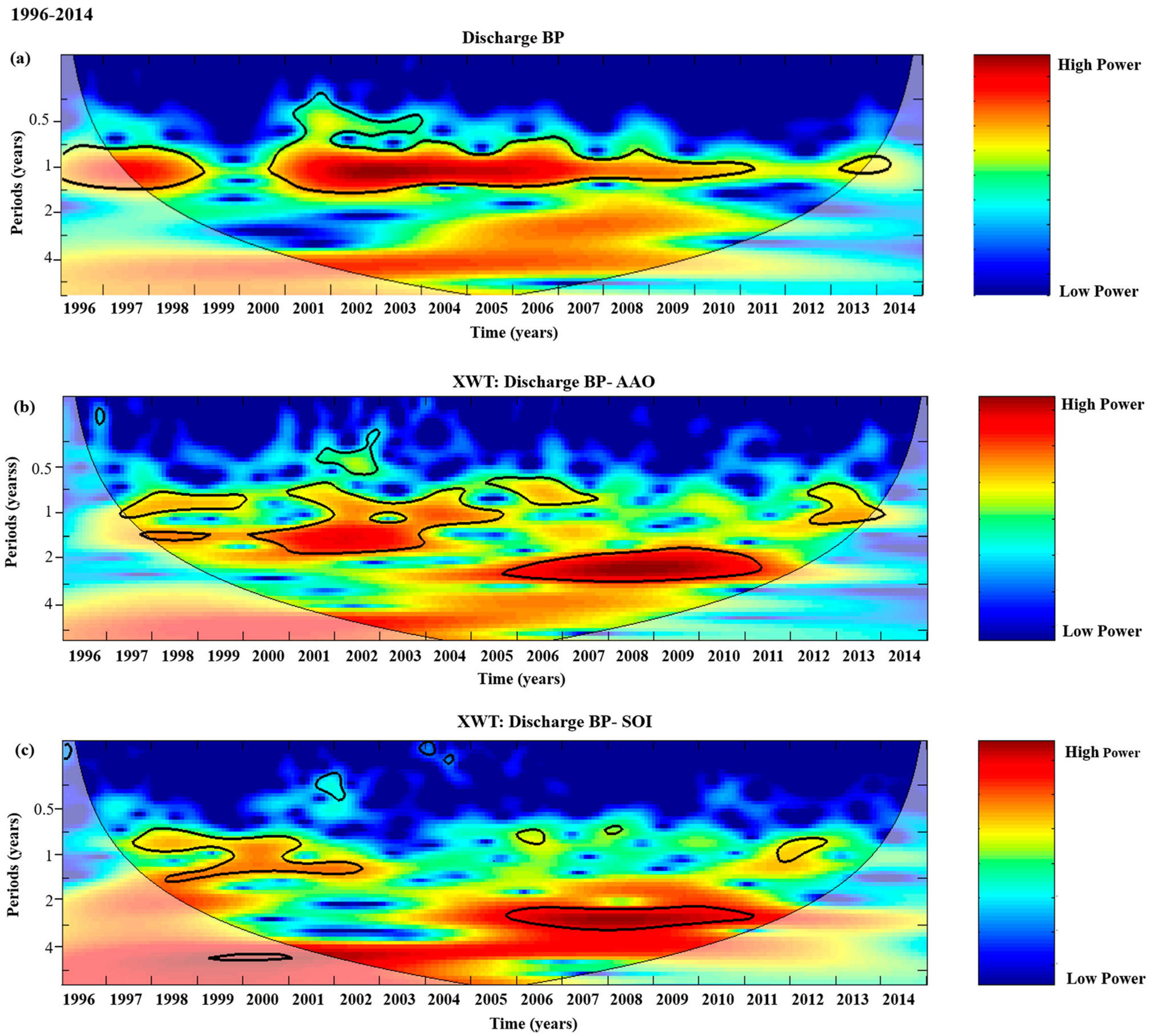

Figure 4. Wavelet analysis of the river discharge measured at the Buen Paso (BP) station, the AAO, and the SOI, during the study period (1996–2014). (a) Wavelets for discharge series showed maximum energy at annual periodicity. Between 1998 and 2000 and between 2010 and 2014 the annual discharge signal disappeared. (b) Cross-wavelets for the river discharge and the AAO series; (c) cross-wavelets for the river discharge and the SOI series. The thick black line designates the 5% significance level compared to red noise, and the shaded area denotes the cone of influence where edge effects may distort the interpretation of that region of time and frequency. The wavelet graphics show how the strength of the periodicities changed over time; colors reflect the squared power of the periodicities (dark red indicates high power; dark blue indicates low power). Cross-wavelet analysis revealed a correlation between river discharge in this region and the AAO at annual and biannual timescales and with the SOI at an annual timescale. During most of the study period, the correlation between river discharge and AAO was strong. The cross-correlation between river discharge and SOI at the annual periodicity was not as consistent as that between discharge and AAO. However, river discharge and SOI were significantly correlated at an annual periodicity between 1999 and 2000 and between 2010 and 2012. These 2 periods coincide with a strong La Niña event (positive SOI) and the disappearance of the annual discharge signal. Thus, the annual discharge seems to have been highly influenced by the AAO. When a strong La Niña event occurred, however, the river discharge was strongly affected.

this correlation practically disappeared after 2001. Discharge and SOI showed a significant correlation at an annual periodicity between 1999 and 2000 and between 2010 and 2012, which coincided with the disappearance of the annual discharge signal. The discharge and SOI were essentially uncorrelated between 2001 and 2005, but between 2006 and 2010 they showed a significant correlation maximum at a period of about 2–3 yr (Fig. 4c).

FFT cross-spectra

The existence of a relationship between the river discharge and the SOI and AAO was also supported by

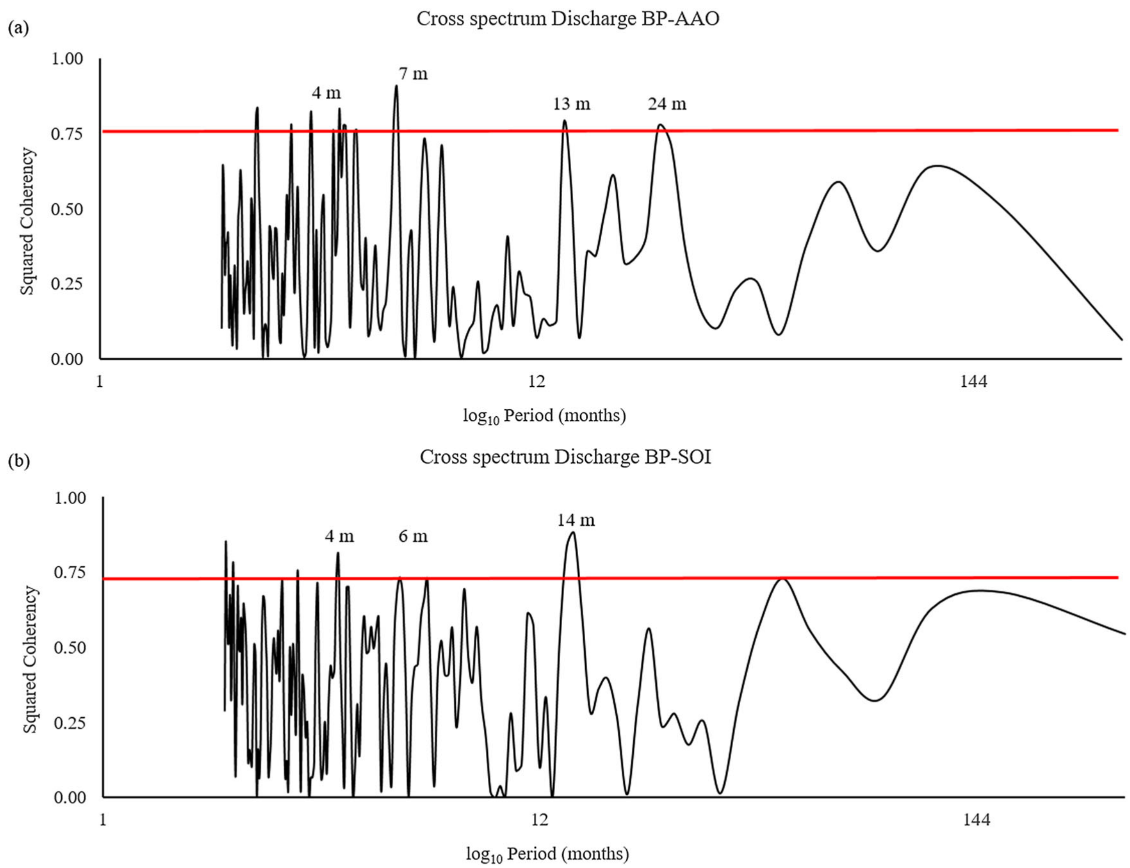

Figure 5. Cross-spectral fast Fourier transform analysis between river discharge measured at the BP station, and both AAO and SOI (during 1987–2014). (a) The squared coherency spectrum between river discharge and AAO shows significant (>0.75) peaks at intraannual (4–7 months), quasi-annual, and every 2 year periods; (b) the squared coherency spectrum between river discharge and SOI shows significant (>0.75) peaks only at intraannual (4–6 months) and quasi-annual periods.

the results of an FFT cross-spectral analysis (Fig. 5). In the squared coherency spectrum, the river discharge and AAO showed significant peaks (>0.75) at intraannual (4–7 months), quasi-annual (13 months), and every 2 year periodicities (Fig. 5a). The same was true of river discharge and SOI at intraannual (4–6 months) and quasi-annual (14 months) periodicities (Fig. 5b).

We also analyzed the phase shift between discharge and both climate indexes. For intraannual periodicities, the discharge lagged the AAO by 1 month and the SOI by slightly <1 month. AAO is the main precipitation driver in the Andes south of 40°, whereas precipitation in the Patagonian plains region is more highly correlated with the SOI than with the AAO (Aravena and Luckman 2009). Precipitation in the upper Andes takes at least a month to be reflected in the river discharge in the lower basin, whereas flow within the lower basin responds almost immediately to precipitation in the Patagonian plains. For the quasi-annual period, the discharge lagged the AAO and SOI by 5–6 months, a time lag that agrees with the basin hydrological regime; snow that falls in the Andes during winter melts during the following spring and summer. Regarding the every 2 year period, the river discharge lagged the AAO by 6 months, possibly associated with the time required for the melting of accumulated snow, which can exceed a year.

Other studies have also shown that the discharge of Patagonian rivers between 30°S and 40°S correlate with ENSO events at decadal, quasi-biennial and interannual frequencies (Compagnucci and Araneo 2007, Pasquini and Depetris 2007, Araneo and Compagnucci 2008). The results presented here are the first, however, to show a relationship between river discharge east of the Andes in the transitional area of 45–50°S and SOI and AAO.

Both climate modes are important and seem to be interacting with the river discharge in this region. The annual river discharge signal was associated with both the annual and every 2 year AAO signals; however, a decrease in the energy of the annual discharge signal was observed during some specific periods (1998–2000 and 2010–2014) that coincided with periods of strong cross-correlation between river discharge and the SOI.

Those periods in which the annual discharge signal disappeared corresponded with periods of low discharge, which finally produced a decrease in the lake surface area.

Relationships between lake surface area and discharge, AAO, and SOI

In both the Musters and Colhué Huapí areas, the river discharge increased (decreased) when it was preceded by negative (positive) AAO and SOI anomalies (Fig. 6). Periods of increasing lake surface area (2001–2007) were preceded by negative AAO and SOI anomalies, whereas periods of decreasing lake surface area (1998–2001 and 2007–2014) were preceded by positive AAO and SOI anomalies (Fig. 6).

Three years of positive AAO and SOI anomalies, with almost no interruption, preceded 2001, when the lake surface area of Colhué Huapí reached its smallest size (Fig. 6). River discharge was affected during those years. The lowest records in the series of both hydrological stations occurred before 2001 (mean annual values: LM = 28.6 m^3/s and BP = 0.6 m^3/s). In 2007 Colhué Huapí Lake reached its largest surface area (797 km^2), preceded by 6 years of mostly positive AAO and SOI anomalies. River discharge records during those 6 years were the highest in the series of both stations (mean annual values: LM = 79.4 m^3/s and BP = 42 m^3/s). During 2007–2015, AAO and SOI anomalies were positive in most years, and the lake surface area decreased.

Discussion

During the study period, interannual fluctuations in lake surface area were more evident in Colhué Huapí Lake than in Musters Lake. Musters is a narrow, deep lake with a tectonic origin and steep sides. Therefore, only notably large variations in lake volume have an appreciable effect on lake surface area. Colhué Huapí, however, is a large, shallow lake, so changes in lake volume are reflected much more strongly in lake surface area.

Both lakes lie at the lowest level of the Senguer River basin, a large and complex hydrological system. Thus, the water balance of the lakes involves discharge from the upper basin but also local factors such as evaporation and precipitation in the lower basin.

The interannual variations in the surface areas of the 2 lakes in a given year can be explained by the joint effect of total annual discharge, total annual precipitation over the lakes, and total annual evaporation from the lakes during the previous year (adjusted R^2: Colhué Huapí = 86% and Musters = 74%). The variation in lake surface area not explained by the multiple regression may be associated with those water fluxes that could not be included in the study due to lack of data (e.g., groundwater flow and water reaching the lakes through return channels after being used for crop irrigation). Further, uncertainty associated with the pixel size of the Landsat images can especially affect the calculation of the surface area of Musters Lake because of its geomorphology. The variation in the surface area of deep lakes is sometimes small and can be difficult to detect with a 30 × 30 m pixel size.

The correlation coefficient associated with the multiple regression for the surface area of Colhué Huapí Lake was higher than that for Musters Lake, explained by a series of anthropogenic impacts that affect Musters Lake more directly than Colhué Huapí Lake. One of these impacts is the effect of agriculture. Before reaching Musters Lake, water must pass through fertile crop land (Sarmiento Valley) located between the 2 lakes, an area with a large number of irrigation channels (Tejedo 2003). About 10 m^3/s of water is used for agricultural activities during the irrigation season (Jul–Dec). Currently, no accurate measurement is available for the percentage of water that remains in the fields; thus, the water discharge into Musters Lake may deviate from the value measured at the LM station because river discharge might be affected by extraction for agricultural use. The BP station, however, is located near Colhué Huapí Lake, an area with few anthropogenic activities.

We observed that local forcing factors, such as precipitation and evaporation, are important in determining interannual variations in the surface areas of the 2 lakes, but river discharge, which is not a local forcing factor, was the most significant determinant. Although discharge levels into the 2 lakes differed with regard to magnitude, their variations were similar. Interannual changes in discharge were driven mostly by snowmelt and precipitation in the Andes and the Patagonian plains. Our results differ from those of other studies, which have emphasized the importance of local forcing factors for lakes in this region (Pasquini et al. 2008).

The literature reports some contradictory results regarding which of the major southern climate modes (AAO or ENSO) is actually driving precipitation in the Andes and, consequently, river discharge, between 45°S and 50°S. Previous studies concluded that river discharge in this area is strongly related to sea surface temperature in the El Niño 3 + 4 area (Compagnucci and Araneo 2007). The Southern Annular Mode, however, is the main climate forcing factor (with a minor influence of ENSO events) on the discharge of the Baker River in Chilean Patagonia (46–48°S; Lara et al. 2015). Other studies discovered that precipitation is reduced by 10–20% during El Niño events on the west coast of Chile between 45°S and 55°S (Schneider and Gies 2004).

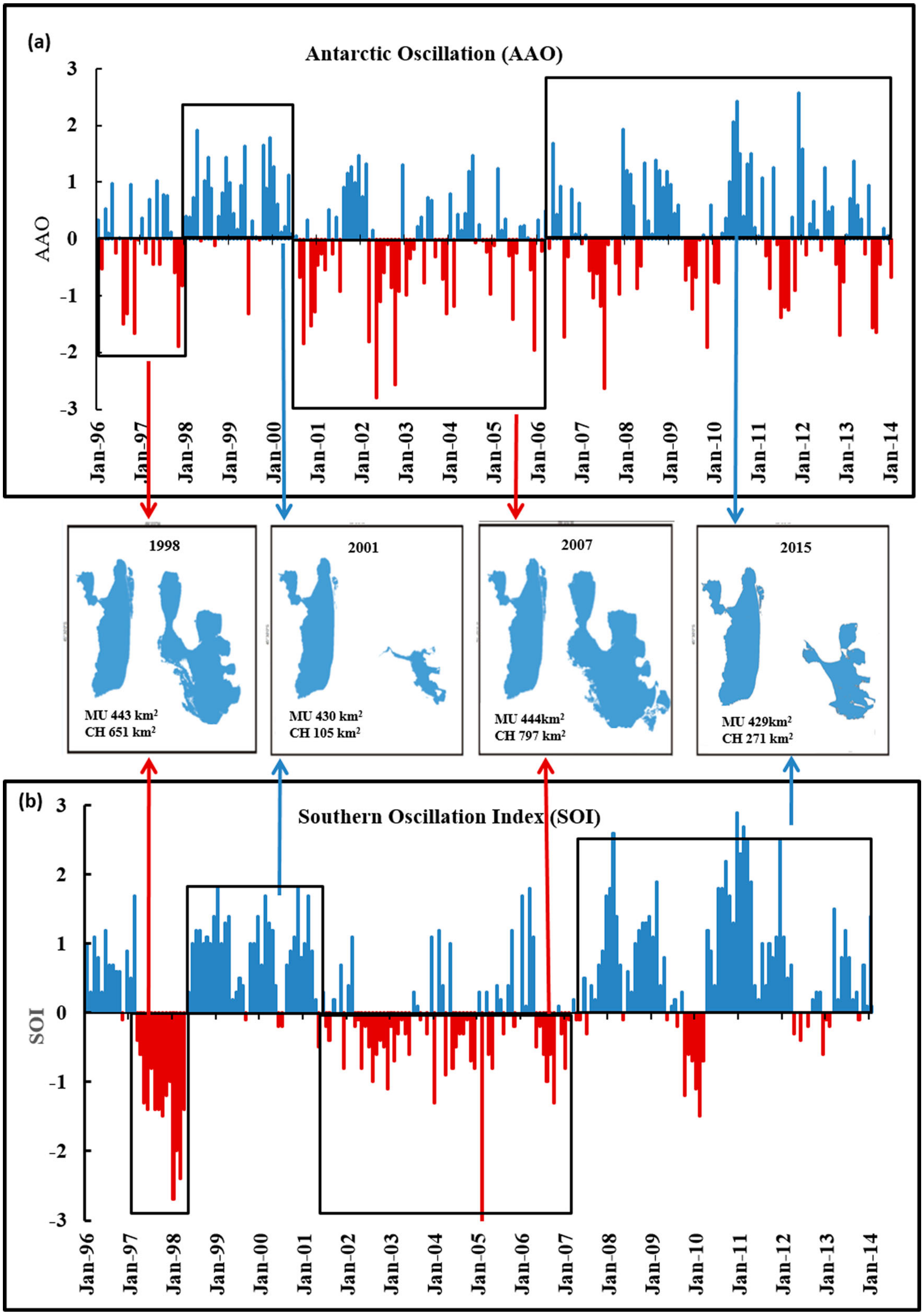

Figure 6. Relationships between 2 southern climate modes (AAO and SOI) and the surface areas of 2 Patagonian lakes, Colhué Huapí (CH) and Musters (MU). (a) Years with mostly negative (positive) AAO values immediately precede years with the largest (smallest) lake surface areas. The AAO affects discharge by increasing or decreasing snow deposition in the upper basin. (b) Years with mostly negative (positive) SOI values also immediately precede years with the largest (smallest) lake surface areas. The SOI affects discharge in the Patagonian plains by increasing or decreasing local precipitation in the lower basin.

We found that variations in both the AAO and the SOI affect river discharge in the Senguer River basin, which eventually affects Musters and Colhué Huapí lakes. Periods of increasing lake surface area were preceded by negative anomalies in both AAO and SOI, which were associated with notably high river discharge rates, whereas periods of decreasing lake surface area were preceded by positive anomalies in both AAO and SOI, which were associated with notably low river discharge rates.

During the study period, river discharge in this region was strongly influenced by the AAO. Strong La Niña events also highly affected the river discharge, however, resulting in a decrease in lake surface area. The wavelet analysis for the discharge showed a strong annual signal over most of the time period analyzed, but during some years (1998–2000 and 2010–2014) this signal disappeared. The existence of a significant correlation maximum at an annual periodicity in the cross-wavelet spectrum supports the hypothesis of a relationship between river discharge and the SOI and AAO. For river discharge and AAO, this relationship was strong during most of the study period. During 1999–2000 and 2006–2012, however, no significant correlation was found at an annual periodicity; instead, an interannual (2–3 yr) signal appeared. The cross-correlation between river discharge and the SOI at an annual periodicity was not as consistent as that between river discharge and the AAO; however, a significant correlation was found between river discharge and SOI at an annual periodicity between 1999 and 2000 and between 2010 and 2012. These 2 periods coincide with a strong La Niña (positive SOI) event and the disappearance of the annual discharge signal.

FFT squared coherency spectra between river discharge and the 2 climate mode indices showed significant peaks at intraannual (4–6 months), quasi-annual, and every 2 year periodicities. Also, the time lag between discharge and both climate indexes agrees with the time lag expected based on the hydrological regime of the basin.

This analysis is the first to focus on the relationship between river discharge east of the Andes in the transitional area of 45–50°S and both the AAO and SOI. Our results agree with those of other regional studies, which found that both AAO and SOI affect the hydrology of Patagonia (Aravena and Luckman 2009). Whereas rainfall in the Patagonian plain is strongly related to the SOI, rainfall and snow accumulation in the Andes are related to the AAO. In a large and complex basin like that of the Senguer River, the effect of both these southern climate modes on the variability of river discharge can be observed.

Although variations in precipitation and evaporation also seem to be significant determinants of fluctuations in the surface area of Colhué Huapí Lake, these factors are much less important for Musters Lake. This difference between the 2 lakes is due mainly to differences in their physical characteristics such as depth, surface area, and geomorphology, but differences in the effect of the wind on the 2 lakes must also be considered. Evaporation from Colhué Huapí Lake, which is shallow and exposed to the predominantly westerly winds, is likely higher than that from Musters Lake, which is sheltered from the wind by elevated terrain (1200 m) on its western, northern, and central-east coasts. Moreover, direct precipitation on to the lake surface is also likely more important for Colhué Huapí Lake, which has a much smaller volume than Musters Lake.

In 2001, the surface area of Colhué Huapí Lake had contracted to the smallest value ever recorded (105 km^2), and some studies predicted that the joint effect of the hydrological deficit in the region and anthropogenic impact would lead to the disappearance of the lake (Coronato 2003, Tejedo 2003). That this has not occurred implies the situation is more complex than assumed. On a global scale, climate change and human activity have affected the location and persistence of many surface waters, which in some cases have disappeared altogether as a result of these factors (Pekel et al. 2016). Our study shows that Colhué Huapí Lake is subject to large fluctuations in surface area, mostly caused by fluctuations in natural variables, especially river discharge. These fluctuations can be traced back at least partially to regional climate variability as represented by climate modes such as the AAO and the SOI. Further research is required to understand completely the impact of human activities on the variability of the surface areas of these lakes.

Conclusions

Interannual variations in the surface areas of 2 Patagonian lakes were analyzed. Multiple regressions, using river discharge, precipitation over the lakes, and evaporation from the lakes as independent variables, were calculated and validated. These multiple regressions allowed us to analyze statistically which of those variables significantly affects the surface areas of the lakes. The statistical analysis showed that river discharge was the main driver of interannual variations in the surface areas of both lakes. Cross-wavelet analysis and FFT cross-spectral analysis revealed that river discharge in this region was especially correlated with the AAO at annual and every 2 year periodicities; however, the presence of strong signals from La Niña events (positive SOI:

1996–2002 and 2007–2014) corresponded with a low discharge, which finally resulted in a decrease in lake surface area.

These results are the first showing the effect of both AAO and SOI on river discharge and lake surface area east of the Andes between 45°S and 50°S. The study provides basic information for understanding how climatic variability affects extra-Andean Patagonian lakes. Additionally, these results are likely to be useful for designing a water resource management plan for the Senguer River basin, an important consideration because Musters Lake (located within the basin) is the source of water for 350 000 inhabitants of the region. Future studies will focus on how to predict variations in lake surface area using the information obtained here on the relationship between river discharge and the AAO and SOI.

Acknowledgements

Partial support for this study was provided by grants from the Inter-American Institute for Global Change Research (IAI) CRN3038, which is supported by the US National Science Foundation (Grant GEO-1128040), and an IAI-CONICET special grant. We also thank the Universidad Nacional del Sur and the Concejo Nacional de Investigaciones Científicas y Técnicas. Thanks are also due to Drs. M. Celeste Lopez Abbate and Alejandro J. Vitale for their support with the methodology employed and to the reviewers and the editor for their comments, which improved the paper.

References

Aceituno P. 1988. On the functioning of the Southern Oscillation in the South American sector. Part I: surface climate. Monthly Weather Review. 116:505–524.

Araneo DC, Compagnucci RH. 2008. Atmospheric circulation features associated to Argentinean Andean rivers discharge variability. Geophys Res Lett. 35:L01805.

Aravena JC, Luckman BH. 2009. Spatio-temporal rainfall patterns in southern South America. Int J Climatol. 29:2106–2120.

ArcGIS. 2010. (Version 10.0). Redlands (CA): ESRI.

Beniston M, Stoffel M. 2014. Assessing the impacts of climatic change on mountain water resources. Sci Total Environ. 493:1129–1137.

Bohn VY, Delgado AL, Piccolo MC, Perillo GME. 2016. Assessment of climate variability and land use effect on shallow lakes. Environ Earth Sci. 75:818.

Bruesewitz DA, Carey CC, Richardson DC, Weathers KC. 2015. Under-ice thermal stratification dynamics of a large, deep lake revealed by high-frequency data. Limnol Oceanogr. 60:347–359.

Bruniard ED. 1992. Hidrografía: procesos y tipos de escurrimiento superficial [Hydrography processes and types of surface runoff]. Buenos Aires (Argentina): Editorial Ceyne. Spanish.

Carey C, Hanson PC, Lathop RC, St. Amand AL. 2016. Using wavelet analyses to examine variability in phytoplankton seasonal succession and annual periodicity. J Plankton Res. 38:27–40.

Chuvieco E. 2010. Teledetección Ambiental. La observación de la tierra desde el espacio [Enviromental teledetection. Earth observation from the space]. Barcelona (Spain): Editorial Planeta S.A. Spanish.

Chopra S, Marfurt KJ. 2015. Choice of mother wavelets in CWT spectral decomposition. 83rd Annual International Meeting, SEG Technical Program. Expanded Abstracts; p. 2957–2961.

Compagnucci RH, Araneo DC. 2007. Alcances de El Niño como predictor del caudal de los ríos andinos argentinos [El Niño as predictor of Argentinean river flow]. Ing Hidraul Mex. 22:23–35. Spanish.

Coronato F. 2003. El problema de la desecación del Lago Colhué Huapí desde la Geografía Histórica [Colhué Huapí Lake drought problem, a view from historical geography]. Actas de la 64ª Semana de Geografía GAEA. p.165–170. Spanish.

Dore MHI. 2005. Climate change and changes in global precipitation patterns: what do we know? Environ Int. 31:1167–1181.

Downing JA. 2010. Emerging global role of small lakes and ponds: little things mean a lot. Limnetica. 29:9–24.

ENVI. 2010. (Version 4.7). Boulder (CO): Harris Geospatial, Research Systems.

George G, Hurley M, Hewitt D. 2007. The impact of climate change on the physical characteristics of the larger lakes in the English Lake District. Freshwater Biol. 52:1647–1666.

González Díaz EF, Di Tommaso I. 2014. Paleogeoformas lacustres en los lagos Musters y Colhué Huapí, su relación genética con un paleolago Sarmiento previo, centro sur del Chubut [Paleo lacustrine landforms in Colhué Huapí and Musters lakes, their genetic connection with a previous Sarmiento paleolake, Central-South Chubut]. Rev Asoc Geol Argentina. 71:416–426. Spanish.

Grinsted A, Moore JC, Jevrejeva S. 2004. Application of the cross wavelet transform and wavelet coherence to geophysical time series. Nonlinear Proc Geophys. 11:561–566.

Holgerson MA, Farr ER, Raymond PA. 2017. Gas transfer velocities in small forested ponds. J Geophys Res Biogeosci. doi:10.1002/2016JG003734

Hondzo M, Stefan HG. 1993. Regional water temperature characteristics of lakes subjected to climate change. Clim Change. 24:187–211.

Horning N. 2004. Selecting the appropriate band combination for an RGB image using Landsat imagery Version 1.0. New York (NY): American Museum of Natural History, Center for Biodiversity and Conservation. Technical report.

Lara A, Bahamondez A, González Reyes A, Muñoz AA, Cuq E, Ruiz Gómez C. 2015. Reconstructing streamflow variation of the Baker River from tree-rings in Northern Patagonia since 1765. J Hydrol. 529:511–523.

Lau KM, Weng H. 1995. Climate signal detection using wavelet transform: how to make a time series sing. Bull Am Meteorol Soc. 76:2391–2404.

Masiokas M, Villalba R, Luckman B, Lascano M, Delgado S, Stepanek P. 2008. 20th-century glacier recession and regional hydroclimatic changes in northwestern Patagonia. Glob Planet Chang. 60:85–100.

MATLAB. 2016. Wavelet Toolbox (version 9.0). MathWorks, Inc.
Milly PCD, Dunne KA, Vecchia AV. 2005. Global pattern of trends in stream flow and water availability in a changing climate. Nature. 438:347–350.
Nash JE, Sutcliffe JV. 1970. River flow forecasting through conceptual models. Part I. A discussion of principles. J Hydrol. 10:282–290.
[NASA] National Aeronautics and Space Administration. 1999. Landsat 7 science data users handbook. https://landsat.gsfc.nasa.gov/wp-content/uploads/2016/08/Landsat7_Handbook.pdf
Pasquini AI, Depetris PJ. 2007. Discharge trends and flow dynamics of South America rivers draining the southern Atlantic seaboard: an overview. J Hydrol. 333:385–399.
Pasquini AI, Lecomte KL, Depetris PJ. 2008. Climate change and recent water level variability in Patagonian proglacial lakes, Argentina. Glob Planet Chang. 63:290–298.
Park JH, Duan L, Kim B, Mitchell MJ, Shibata H. 2010. Potential effects of climate change and variability on watershed biogeochemical processes and water quality in Northeast Asia. Environ Int. 36:212–225.
Pekel JF, Cottam A, Gorelick N, Belward AS. 2016. High-resolution mapping of global surface water and its long-term changes. Nature. 540:418–422.
Quirós R. 1988. Relationships between air temperature, depth, nutrients and chlorophyll in 103 Argentinian Lakes. Verh Internat Ver Limnol. 23:647–658.
Quirós R, Delfino R, Cuch S, Merello R. 1983. Diccionario Geográfico de Ambientes Acuáticos Continentales de la República Argentina. Parte I: Ambientes Lénticos [Geographic dictionary of continental aquatic environments of the Argentine Republic. Part I: Lentic environments]. Instituto Nacional de Investigación y Desarrollo Pesquero (INIDEP) Departamento de Aguas Continentales; 475 p.
Quirós R, Drago E. 1999. The environmental state of Argentinean lakes: an overview. Lakes Reserv Res Manage. 4:55–64.
Read JS, Hamilton DP, Desai AR, Rose KC, MacIntyre S, Lenters JD, Smyth RL, Hanson PC, Cole JJ, Staehr PA, et al. 2012. Lake-size dependency of wind shear and convection as controls on gas exchange. Geophys Res Lett. 39:L09405.
Schneider C, Gies D. 2004. Effects of El Niño-Southern Oscillation on southernmost South America precipitation at 53°S revealed from NCEP-NCAR reanalyses and weather station data. Int J Climatol. 24:1057–1076.
Scordo F, Seitz C, Zilio M, Melo WD, Piccolo MC, Perillo GME. 2017. Evolución de los recursos hídricos en el “Bajo de Sarmiento” (Patagonia extra andina). Análisis integrado de los procesos naturales y del impacto antrópico [Evolution of water resources in the “Bajo de Sarmiento” (Extraandean Patagonia): natural and anthropogenic impacts]. Anuario do Instituto de Geociências. 40:106–117.
Shi YF, Ren JW. 1990. Glacier recession and lake shrinkage indicating a climatic warming and drying trend in central Asia. Ann Glaciol. 14:261–265.
Shimoda Y, Azim ME, Perhar G, Ramin M, Kenney MA, Sadraddini S, Gudimov A, Arhonditsis GB. 2011. Our current understanding of lake ecosystem response to climate change: what have we really learned from the north temperate deep lakes? J Great Lakes Res. 37:173–193.
Statistica. 2002. StatSoft (version 7). http://www.statsoft.com/Products/STATISTICA-Features
[SSRH] Subsecretaría de Recursos Hídricos de la Nación Argentina. 2016. Base de datos hidrológica integrada [Hydrological integrated database]. http://www.hidricosargentina.gov.ar/acceso_bd.php. Spanish.
Tejedo AG. 2003. Degradación de suelos en los alrededores del lago Colhué Huapí, Escalante, provincia de Chubut [Soil degradation around Colhué Huapi Lake, Escalante, Chubut province]. Primer Congreso de la Ciencia Cartográfica y VII Semana Nacional de la Cartografía. Buenos Aires. Spanish.
Torbick N, Ziniti B, Wu S, Linder E. 2016. Spatiotemporal lake skin summer temperature trends in the Northeast United States. Earth Interact. 20:1–21.
Torrence C, Compo GP. 1998. A practical guide to wavelet analysis. Bull Am Meteorol Soc. 79:61–78.
Valladares A. 2004. Cuenca de los ríos Senguer y Chico [Senguer and Chico rivers basin]. Argentina: Informe Técnico Subsecretaria de Recursos Hídricos de la Nación. Spanish.
Whitehead PG, Wilby RL, Battarbee RW, Kernan M, Wade AJ. 2009. A review of the potential impacts of climate change on surface water quality. Hydrolog Sci J. 54:101–123.
Williamson CE, Dodds W, Kratz TK, Palmer MA. 2008. Lakes and streams as sentinels of environmental change in terrestrial and atmospheric processes. Front Ecol Environ. 6:247–254.
Williamson CE, Saros JE, Vincent WF, Smol JP. 2009. Lakes and reservoirs as sentinels, integrators, and regulators of climate change. Limnol Oceanogr. 54:2273–2282.
Woolway RI, Maberly SC, Jones ID, Feuchtmayr H. 2014. A novel method for estimating the onset of thermal stratification in lakes from surface water measurements. Water Resour Res. 50:5131–5140.
Woolway RI, Jones ID, Maberly SC, French JR, Livingstone DM, Monteith DT, Simpson GL, Thackeray SJ, Andersen MR, Battarbee RW, et al. 2016. Diel surface temperature range scales with lake size. PLOS ONE. 11:e0152466.
Woolway RI, Meinson P, Nõges P, Jones ID, Laas A. 2017. Atmospheric stilling leads to prolonged thermal stratification in a large shallow polymictic lake. Clim Change. 141:759–773.
Yan L, Zheng M. 2015. The response of lake variations to climate change in the past forty years: a case study of the northeastern Tibetan Plateau and adjacent areas, China. Quat Int. 371:31–48.
Ye Q, Yao T, Chen F, Kang, S, Zhang X, Wang Y. 2008. Response of glacier and lake covariations to climate change in Mapam Yumco Basin on Tibetan Plateau during 1974–2003. J Glaciol. 52:537–545.